Influence of Morphology on Radio Frequency Human exposure.

Joe Wiart *senior member IEEE*, Emmanuelle Conil, Aimad El Habachi, Abdelhamid Hadjem and Man-Faï Wong *senior member IEE.*

Orange labs RD Issy les Moulineaux France
Joe wiart@orange-ftgroup.com

Abstract—

Several studies have been conducted to assess the Whole Body Specific Absorption Rate induced by exposure to plane wave. In this paper we analyse the whole body power absorbed and the relationship with the body surface area. Different voxels whole body models of adult, based on MRI, are used. Using morphing techniques child models are also used. The power absorbed by these phantom expose to a plane wave is estimated using the finite difference in time domain method. The direction of arrival of the plane wave is front to the phantoms and the frequency is 2.1 GHz. The Absorbed Body Cross Section (ABCS) and the Radiated Body Cross Section are studied

.

Key words: SAR, FDTD, plane wave, cross section. EMF

I. INTRODUCTION

THERE is a public concern about possible health effects of Radio Frequency (RF) exposure and the increasing use of electromagnetic field (EMF) in wireless technologies increases such concern. The relationship between the incident field and the whole body specific absorption rate (WBSAR) has been investigated to protect general public from overexposure. The first numerical studies have used simplified human models. Today the computers have been improved and are able to handle large problems. Taking advantage of such improvement the relationship between the incident field and the WBSAR has been revisited using new voxel models of humans [1][[2][3][4][5][6][7][8][9][10][11]. These studies have shown a large variability [9]. In this paper, we will focus on the influence of the morphology on the total power absorbed. Absorbed Body Cross Section (ABCS) and Radiated Body Cross Section (RBCS) are defined. ABCS is given by the total power absorbed by the body divided by the incident power density (IPD). RBCS is given by the Radiated power of the body divided by the IPD. We will analyse the relation between

II. METHOD AND MODELS

A. Phantoms

Worldwide several human phantoms models have been developed and described in several publications [1-8]. Visible human [6] has been used intensively but other phantoms have been developed such the Japanese male and female [3], the UK male and female [4][5], the Korean models [2][7], the zubal model [8]. Recently the virtual family (2 adult models and 2 child models) have been also developed [1]. In this study we will used 8 of these model: the adults (Ella and Duke) of the virtual family models, the UK male model (Norman), the Korean model of ETRI, the Japanese model , the Zubal model and the Visible Human model.. Some of them are shown in Figure 1. The resolution of these human body models varies from 1 millimetre to 3.6 mm.

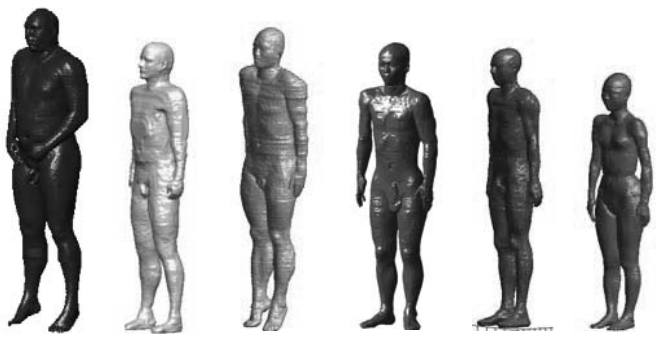

Figure 1 Some models used in this study (VH, Zubal,Korean M, Japanese M, Norman, Japan F)

As shown in figure 2, depending on the phantoms the mass percentage of tissues vary. For instance the mass percentage of skin can vary from 5% to 12%. The difference can be due

to the morphology but it can also be induced by the different voxel size.

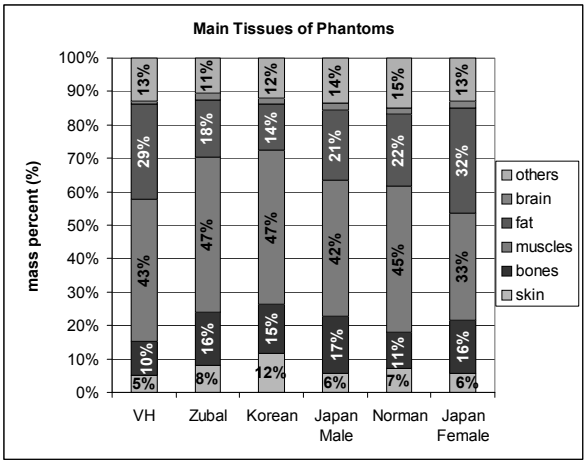

Fig. 2 Variability of phantom morphology of phantoms

Since there are not a lot of children phantoms, morphing techniques [12] have been developed and used in several studies. Based on piecewise downscaling such technique allows to generate new phantoms providing that external body size are known. It allows distorting external morphology by homothetic deformation assuming that the external morphology retains the same proportionality in terms of age. Figure 3 shows the 5 years old child model derived from Norman.

Figure 3 5 years old child model derived from Norman using morphing techniques.

B. Numerical method

The SAR is estimating using the phantoms the well known Finite Difference Time Domain (FDTD). This method has been used since it has demonstrated its advantages in many EMF problems [13]. With this method the field E and H are discretized in both space (see fig 4) and time using the Yee scheme [14].

To avoid spurious reflection at the boundary of the computational domain the well known Perfectly-Matched Layer [15].

The FDTD code has been developed in our laboratories and tested many time. In our code we have developed routine allowing to use Huygens box and to calculate near to far field, Local SAR over 10g, power re-radiated.

The SAR is computed using the usual formulation:

$$SAR = \frac{\sigma E^2}{\rho} \qquad \mathbf{1}$$

Where σ, ρ and E are respectively the conductivity, the mass density and the rms E field strength.

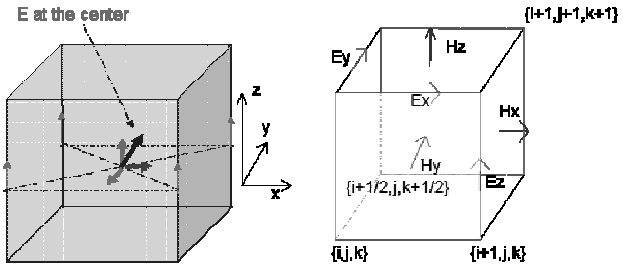

Figure 4 Yee cell (right) and the E field a the center of the cell (left)

The Whole body SAR is given by the summation of power absorbed in each voxel divided by the total mass of the phantom.

III. Results

A Absorbed Body Cross section.

At frequencies above the human resonance the power absorbed can depend on the equivalent body surface. Based on adult MRI based models different child have been created. The WBSAR has been estimated in case of exposure to a plane wave at 2.1 GHz. The relationship between BSA [16] or BMI and WBSAR has been analysed [11]. Depending on the phantom the ratio between absorbed power and BSA*IPD (where IPD is the Incident Power Density) can vary from 0.159 to 0.2794. For all the phantoms the Projected Body Surface Area (PBSA) has been also estimated, the PBSA is obtained by projection of the body phantom on a plane orthogonal to the incident field. Depending on the phantom the ratio between absorbed power and PBSA*IPD (where IPD is the Incident Power Density) can vary from 0,523 to 0.930.

Model	Pabs/ (PBAS*IPD)	Pabs/ (BSA*IPD)
Norman Male (Uk)	0,868	0,265
Japan Male	0,930	0,280
Korean Male	0,523	0,159
Zubal Male (Us)	0,693	0,197
VH Male (Us)	0,787	0,197
Japanese Female	0,892	0,275
Ella Female (Ch)	0,921	0,275
Duke Male (Ch)	0,823	0,248

Table 1: Pabs/ (PBAS*IPD) and Pabs/ (BSA*IPD) vs the body models.

For all the models the Absorbed Body Cross Section (ABCS) can also be estimated and compared to the PBSA. The Absorbed Body Cross section is given by the Body absorbed power divided by the incident power density

Model	ABCS	PBSA	ABCS/PBSA
Norman Male (Uk)	0,474	0,546	0,868
Japan Male	0,504	0,542	0,930
Korean Male	0,313	0,598	0,523
Zubal Male (Us)	0,391	0,563	0,693
VH Male (Us)	0,491	0,623	0,787
Japanese Female	0,423	0,474	0,892
Ella Female (Ch)	0,446	0,484	0,921
Duke Male (Ch)	0,461	0,560	0,823

Table 2: ABCS , PBSA and the ration ABCS/PBSA versus the different body models.

As it can be seen the ABCS is close to the PBSA but is not equal. Because of that we investigate the absorbed and radiated power of the body

B Body Cross Section of a box

In order to analyse the relationship between the incident power density and the absorbed plus the radiated power a box filled by different tissues has been used. The size of the box is 1.8m*0.6m*0.4m, and the incident field has a polarisation line up with the larger dimension of the box. The incident power density is 0.0013 W/m² at 2100MHz.. The PBSA is in this case equal to 1.08 m²

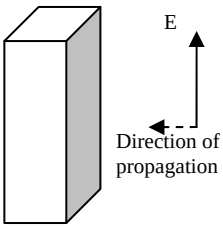

Figure 4 Box exposed

We analyse the ABCS but also the Radiated Body Cross Section (RBCS). Using a Huygens box the power re-radiated by a structure exposed to an incident field can be easily estimated [13]. We have developed such facilities in our FDTD code. Based on that, the Radiated power of the body divided by the incident power density (RBCS) can be estimated.

The box has been filled by different media. HoB1 and HoB2 are filled by an homogeneous media having a sigma of 1.49 S/m and respectively a relative epsilon of 39,8 and 49.8. The third case HoB3 has considered a box filled by a highly lossy dielectric (sigma 2.9e5 s/m and relative epsilon of 39,8). The last case HoB4 has considered a box filled by a multilayer structure composed of skin, fat, muscle and IEC equivalent liquid).

	HoB1	HoB2	HoB3	HoB4
ABCS (m²)	0.615	0.574	1 e-8	0.74
RBCS (m²)	2.46	2.46	3.08	2.308
BCS=ABCS+RBCS	3.015	3.034	3.08	3.048

Table 3 ABCS and RBCS vs case obtained at the frequency of 2.1 GHz

As shown in the table 3 the sum of ABCS and RBCS is about constant whatever is the equivalent liquid used to fill the box. The shape seems to govern the BCS while the ratio between ABCS and RBCS is depending on the media in the box. Since such behaviour can depend on the case we do the same analysis with the child model derived from Norman (see fig 3). A first model NCM1 has been filled with a liquid having a conductivity of 1.49 S/m and a relative epsilon of 39,8. A second model NCM2 has been filled with very highly lossy dielectric (sigma 2.9e5 s/m and relative epsilon of 39,8). NCM2 as HoB are metal models.

	NCM1	NCM2
ABCS (m²)	0,15	0,00
RBCS (m²)	0,35	0,49
BCS=ABCS+RBCS	0,50	0,49

Table 4 ABCS and RBCS vs NCM1 and NCM2 obtained at the frequency of 2.1 GHz

The table 4 confirms the results obtained with the box: the body cross section depends on the shape (box and Norman based Child Model) but not on the material inside the model.

IV. CONCLUSION

In this paper the relationship between the total absorbed power and the incident power has been analyzed. The shape seems to govern the BCS while the ratio between ABCS and RBCS is depending on the media in the box. Such conclusion must be confirmed by additional studies. Future works will concern on the one hand the influence of the media on the relationship between the absorbed power and the BCS, on the other hand future works will also analyse the influence of parameter such height, width of the phantom on BCS.

ACKNOWLEDGMENTS

This study is performed under This work was supported in part by the French ANR project MULTIPASS (http://multipass.elibel.tm.fr/).

The authors would like to thank Dr S Watanabe from NICT, Japan; Dr A K Lee from ETRI, Korea, Dr P J Dimbylow from HPA, UK; Dr P Mason, Dr J Ziriax from Brook'AF, US, Dr N. Kuster from ITIS, CH and Professor Zubal from Yale University, USA, for providing human body models.

REFERENCES

[1] ItisFoundadion http://www.itis.ethz.ch/index/index_humanmodels.html

[2] Lee Ae-K., Choi W.Y., Chung M.S., Choi H.-d, and Choi J., 2006 Development of Korean Male Body Model for Computational Dosimetry, *ETRI Journal*, vol.28, no.1, pp.107-110

[3] Nagaoka T, Watanabe S., Sakurai K., Kunieda E., Watanabe S., Taki M. and Yamanaka Y. 2004 Development of realistic high-resolution whole-body voxel models of Japanese adult males and females of average height and weight, and application of models to radio-frequency electromagnetic-field dosimetry *Phys. Med. Biol* **49** 1-15

[4] Dimbylow P.J. 1996 The development of realistic voxel phantoms for electromagnetic field dosimetry *Proc Int. Workshop on Voxel Phantom Development (National Radiological Protection Board Report)*1-7

[5] Dimbylow P.J. 2005 Development of the female voxel phantom, NAOMI and its application to calculations of induced current densities and electric fields from applied low frequency magnetic and electric fields *Phys. Med. Biol.* **50** 1047-1070

[6] Ackerman MJ. 1995 Accessing the Visible Human Project *D Lib Mag* http://www.nlm.nih.gov/research/visible/visible_human.html

[7] Kim C.H., Choi S.H., Jeong J.H., Lee C. and Chung M 2008.S HDRK-Man: a whole-body voxel model based on high-resolution color slice images of a Korean adult male cadaver *Phys. Med. Biol.* **53** 4093-4106

[8] Zubal I.G., Harrell C.R., Smith E.O., Smith A.L. 1995 Two dedicated voxel-based anthropomorphic (torso and head) phantoms *Proc. of the Int. Conf. at the National Radiological Protection Board*, pp105-111

[9] Conil E., Hadjem A., Wong MF, Wiart 2008 J. Variability analysis of SAR from 20MHz to 2400MHz for different adult and child models using FDTD *Phys. Med. Biol.* **53** 1511-1525.

[10] Dimbylow P J 2002 Fine resolution calculations of SAR in the human body for frequencies up to 3 GHz *Phys. Med Biol.* **47** 2835–46

[11] Hirata A, Kodera S, Wang J and Fujiwara O 2007 Dominant factors influencing whole-body average SAR due to far-field exposure in whole-body resonance frequency and GHz regions *Bioelectromagnetics* **28** 484–7

[12] Abdelhamid Hadjem, David Lautru, Christian Dale, Man Faï Wong, Victor Fouad Hanna, Joe Wiart Study of Specific Absorption Rate (SAR) Induced in the Two Child Head Models and Adult Heads Using a Mobile Phones IEEE Trans. MTT / Microwave Theory and Techniques ; Vol.°53 ; N° 1 ; janvier 2005 ; pp. 4-11.

[13] Taflove A & Hagness S, Computational Electrodynamics. Artech House Ed. 2000 ISBN isbn 1-58053-076-1

[14] Yee K S, 1966 Numerical solution of initial boundary value problems involving Maxwell's equations in isotropic media. IEEE Trans. Antennas Propagat., vol. 14, no. 3, pp. 302-307.

[15] Berenger JP. 1994. A perfectly matched layer for the absorption of electromagnetic waves. J Comput Phys 4:185–200.

[16] DuBois D & DuBois EF 1916 A formula to estimate the approximate surface area if height and weight be known Arch Int Med 17:863-71